

Van-Hove tuning of Fermi surface instabilities through compensated metallicity

Hendrik Hohmann,^{1,2} Matteo Dürrnagel,^{1,2,3} Matthew Bunney,^{4,5}
 Tilman Schwemmer,¹ Titus Neupert,⁶ Stephan Rachel,^{2,4} and Ronny Thomale^{1,2,*}

¹*Institute for Theoretical Physics and Astrophysics,
 University of Würzburg, D-97074 Würzburg, Germany*

²*Würzburg-Dresden Cluster of Excellence ct.qmat, Germany*

³*Institute for Theoretical Physics, ETH Zürich, 8093 Zürich, Switzerland*

⁴*School of Physics, University of Melbourne, Parkville, VIC 3010, Australia*

⁵*Institute for Theoretical Solid State Physics, RWTH Aachen University, 52062 Aachen, Germany*

⁶*Department of Physics, University of Zürich, Winterthurerstrasse 190, Zurich, Switzerland*

(Dated: December 14, 2023)

Van-Hove (vH) singularities in the vicinity of the Fermi level facilitate the emergence of electronically mediated Fermi surface instabilities. This is because they provide a momentum-localized enhancement of density of states enhancing selective electronic scattering channels. High-temperature topological superconductivity has been argued for in graphene at vH filling which, however, has so far proven inaccessible due to the demanded large doping from pristine half filling. We propose compensated metallicity as a path to unlock vH-driven pairing close to half filling in an electronic honeycomb lattice model. It is enabled through the strong breaking of chiral symmetry from intra-sublattice hybridization, leading to the emergence of a hole pocket (hp) nearby the van-Hove points M at the Brillouin zone boundary and an electron pocket (ep) around the zone center Γ . While the ep is radially symmetric and barely contributing to the electronic ordering selection, the hp is dominated by its vH signature and yields electronic order at elevated scales.

Introduction At sufficiently low temperature, metals as interacting many-body electron systems tend to seek a minimization of ground state energy through symmetry breaking. Starting from a Fermi surface (FS) configuration, the metal can become unstable upon the formation of electronic order related to magnetism, charge order, superconductivity, nematicity, and more. Already from earliest descriptions of electronic collective phenomena such as the Stoner criterion for itinerant ferromagnetism or BCS superconductivity, the propensity for FS instabilities generically depends on the ordering's channel-specific coupling strength and the density of states (DoS) at the Fermi level [1, 2]. The latter is intuitive from a Hamiltonian spectral flow perspective: The more spectral weight is pushed away from the Fermi level the more the ground state can be pushed down in energy. Van-Hove singularities (vHs) at or close to the Fermi level are particularly useful to elevate instability scales of electronic order, and are a crucial ingredient to theories of electronic materials. While the clean limit of vHs in two spatial dimensions features a logarithmically diverging DoS at specific points in momentum space, their realization in an imperfect quantum electronic material still ensures a peak in DoS at the vH points.

As many electronic kinetic models naturally feature vH points, it is particularly desirable to devise ways to tune the vH points of a given band structure to the Fermi level in order to facilitate the emergence of vH-driven FS instabilities. Pressure has some tuning impact on vH points, but also implies side-effects to electronic bands some of which would reduce the FS instability scales by reducing the interaction vs. bandwidth ratio [3]. Doping is another established way of tuning the vH profile. Unless

it is constrained to a few percent of doping that could be accomplished via electrolytic gating, however, chemical doping likewise has negative side-effects on FS instability scales such as the enhancement of disorder [4–6].

In this Letter, we propose an alternative principle to perform vH engineering in a model of interacting electrons on the honeycomb lattice. Rather than external pressure or doping, we propose compensated metallicity to deform a Fermi pocket towards the vH points around pristine half filling. We show how the breaking of chiral symmetry facilitates the emergence of a circular electron pocket (ep) at the Brillouin zone (BZ) center and an enlarged hole pocket (hp) tuned into proximity to the vH points at M . While the scattering vertex contributions of the ep turn out to be of marginal significance due to its isotropic character, the vH-proximitized hp triggers ideal conditions for the unfolding of unconventional FS instabilities.

Honeycomb Hubbard model To illustrate vH-tuning assisted by compensated metallicity, we study the t_1 - t_2 - U tight-binding Hubbard model on the honeycomb lattice

$$\hat{H} = \left(-t_1 \sum_{\langle i,j \rangle \sigma} \hat{c}_{i\sigma}^\dagger \hat{c}_{j\sigma} - t_2 \sum_{\langle\langle i,j \rangle\rangle \sigma} \hat{c}_{i\sigma}^\dagger \hat{c}_{j\sigma} \right) + \text{h.c.} \\ - \mu \sum_{i\sigma} \hat{n}_{i\sigma} + U \sum_i \hat{n}_{i\uparrow} \hat{n}_{i\downarrow}, \quad (1)$$

where $\hat{c}_{i\sigma}^{(\dagger)}$ denotes electron annihilation (creation) operators at site i with spin σ and $\hat{n}_{i\sigma} = \hat{c}_{i\sigma}^\dagger \hat{c}_{i\sigma}$, $U > 0$ is the onsite Coulomb repulsion, and μ denotes the chemical potential. The (next) nearest neighbor hopping elements t_1 (t_2) > 0 are visualized in Figure 1(a) as to how they realize (intra-) inter-sublattice hybridization.

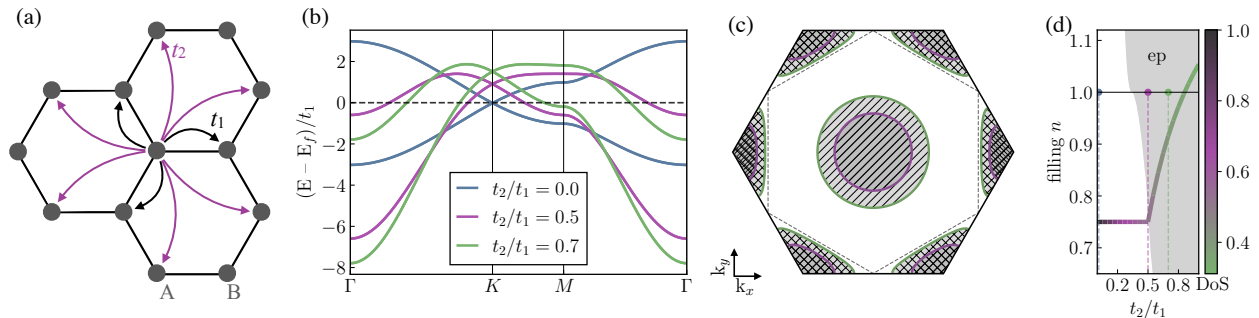


Figure 1. *Chiral symmetry breaking and compensated metallicity* (a) Real space lattice structure and hybridization elements of the honeycomb Hubbard model, as given in Eq. 1. (b) Single particle dispersion of the kinetic terms of Eq. 1. Finite next-nearest neighbor hybridization breaks particle-hole symmetry and shifts the lower van-Hove singularity towards the Fermi level. (c) Fermi surfaces at half filling within the hexagonal BZ, corresponding to the t_2/t_1 hopping values shown in (b). Electron (hole) pockets are indicated by crossed (diagonal) hatching. The perfectly nested outer FS is indicated by dashed line. (d) Lower vH filling and associated DoS at the Fermi level as a function of t_2/t_1 . The opening of the electron pocket around Γ (gray) shifts the vH towards pristine half filling ($n = 1$).

Eq. 1 provides an effective model for graphene monolayers [7, 8]. Diagonalizing the kinetic part of Eq. 1 in the limit $t_2 \ll t_1$, where there is only orbital hybridization between the p_z orbitals of neighboring carbon atoms, a large nested Fermi pocket is realized at van-Hove fillings $n = 3/4, 5/4$, with a point-like FS hosting Dirac points at half filling $n = 1$. These values are pinned by the chiral symmetry of the bipartite honeycomb lattice, $\{\hat{H}, \hat{C}\} = 0$, where $\hat{C} = \hat{P} \cdot \hat{T}$ is defined as the combination of particle-hole (\hat{P}) and time-reversal (\hat{T}) symmetry and can be represented as the third Pauli matrix acting on the sublattice degree of freedom in Eq. (1) [9]. The chiral symmetry of the energy spectrum is broken by imposing finite intra-sublattice hybridization t_2 in Figure 1(b).

Due to the high quality of graphene samples, where lattice distortions or vacancies are rare, the clean limit given in Eq. (1) bears significant resemblance to the experimental setting. A major factor inhibiting the observation of a FS instability in graphene is the small DoS around pristine filling. Tuning graphene to a vH level is therefore an alluring path towards enhancing electronic order, and has been extensively discussed in the literature as a route to promote electronically mediated pairing [10–15]. It is expected to yield a chiral d -wave gapped superconductor, which is a topologically ordered quantum many-body state, *i.e.*, a Chern-Bogoliubov band insulator with Majorana edge modes [16–18]. The realization of such a state has, however, thus far been elusive, since homogeneously doping graphene to such high fillings unavoidably induces a critical amount of disorder to suppress such desired electronic instabilities [4, 5].

Van-Hove tuning from compensated metallicity As opposed to the single pocket case, a multi-pocket fermiology can enable the transfer of charges between Fermi sheets with electron and hole character, in compliance with the Luttinger theorem [19, 20]. In the last decade, this has

been extensively discussed in the case of the iron pnictides [21–23]. In such compounds, an increase of the number of conduction band electrons is compensated for by increasing the occupation of hole states in the valence band. This creates a compensated metal – an overall charge neutral compound with a large ensemble of low-energy hole-type and electron-type excitations at pristine filling, and possibly enhanced nesting effects between eps and hps at and off the Fermi level [24–26].

We find that a key step along the path towards compensated metal phases in a honeycomb lattice model described by Eq. 1 is the assumption of sizable t_2 , which creates an asymmetry between the two vHs (Figure 1(b)). The energy bands are flattened and pushed up in energy at the BZ boundary, while significant t_2 exhibits the opposite effect around the BZ center Γ , introducing an electron pocket at half-filling for $t_2 > t_1/3$. By inducing this Lifshitz transition, we allow the point-like FS of the Dirac point to grow and expand around K , eventually approaching a perfectly nested FS coinciding with the lower vHs for $t_2 \sim 0.85 t_1$ (Figure 1(c)). This respects the Luttinger theorem, as in a multi-pocket scenario of hole-type and charge-type excitations occupied states can be transferred between the pockets while keeping the total electron number constant. Holes in the lower band around K are created by shifting the electrons into the upper band at the BZ center. We can interpret t_2 as a pocket-dependent chemical potential shift, since adjusting t_2 has an effective doping effect on the pocket at the BZ boundary.

Electronic response at vH filling The combined effect of electronic availability of the vHs and nesting features present on the FS determine viable electronic fluctuation channels, manifest in the static electronic response

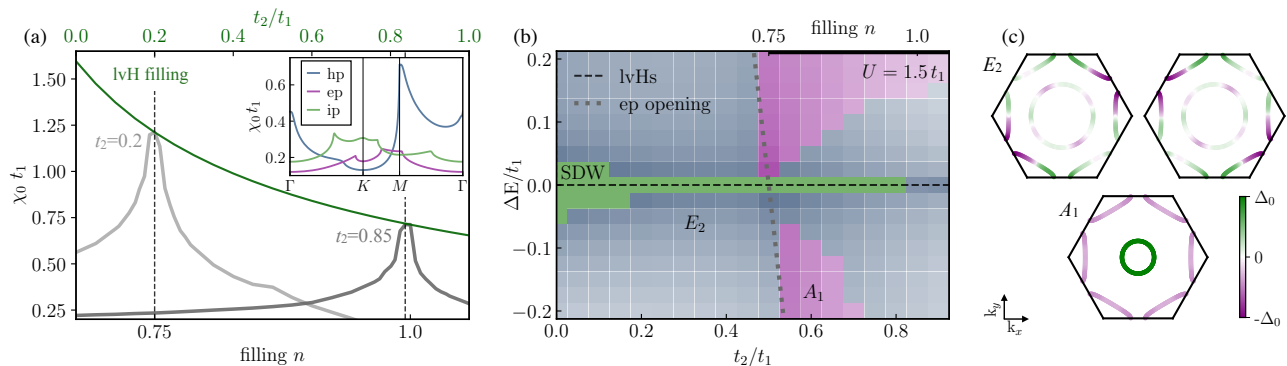


Figure 2. *Many body analysis at lower van-Hove singularity.* (a) Leading eigenvalue of the bare susceptibility χ_0 (Eq. (2)). Both the dependence on t_2 along lower van-Hove (lvH) filling and the doping dependence at fixed long range hopping is depicted. The inset shows the full band-resolved fluctuation spectrum including intra-pocket (ep and hp) and inter-pocket (ip) contributions at $t_2 = 0.85 t_1$ and $n = 1.0$. (b) Resulting phases for Fermi level detuning ΔE from lvHs at intermediate interaction scale $U = 1.5 t_1$. The intensity of the color indicates the SC pairing strength, which is proportional to the transition temperature T_c . (c-d) Superconducting gaps of the chiral d -wave (E_2) and s_{\pm} (A_1), respectively. All calculations were performed with (800×800) integral points and an inverse temperature $\beta = 250/t_1$ to obtain converged results.

function

$$\chi_{o_1 o_2 o_3 o_4}^0(\mathbf{q}) = -\frac{1}{\beta} \sum_n \int_{\text{BZ}} \frac{d\mathbf{k}}{V_{\text{BZ}}} G_{o_2 o_4}(\mathbf{k}, \omega_n) G_{o_3 o_1}(\mathbf{k} + \mathbf{q}, \omega_n) + \text{h.c.} \quad (2)$$

for the screening of the Coulomb interaction. Here, $G_{o_1 o_2}(\mathbf{k}, \omega_n)$ is the single particle propagator with momentum \mathbf{k} , fermionic Matsubara frequency ω_n and additional generalized quantum numbers o_i , incorporating spin and sublattice degrees of freedom. The sum over all frequencies and momenta is normalized by the inverse temperature $\beta = (k_B T)^{-1}$ and the BZ volume.

The primary contributions to the susceptibility are made by states close to the Fermi level, which means that χ^0 can be split into three contributions: intra-ep, intra-hp, and ep-hp inter-pocket (ip) scattering channels. We depict this contribution-resolved susceptibility for the example case $t_2 = 0.85 t_1$ in the inset of Figure 2(a), which is where the vH filling approaches half filling $n = 1.0$. The emerging pocket around Γ is a circular ep, where the near isotropy does not promote any distinct transfer momenta \mathbf{q} . This manifests itself as an absence of distinct peaks in the electronic response [10, 27]. Unlike the Fermiology of pnictides, no nesting exists between the two FS sheets, such that inter-pocket scattering processes are marginal. Hence the dominant fluctuations are exclusively located in the intra-hp scattering channel, where the vHs tuning provides a large DoS to participate in the electronic ordering at the Fermi level, which is concentrated at the M points of the hexagonal BZ. Accordingly, fluctuations with wavevector $\mathbf{q} = M$ contain scattering events with high occupancy of the initial and final states, and thus provide the low-lying fluctuations in the system.

We depict the strength of M point electronic fluctua-

tions $\chi^0(M)$ at lower van-Hove (lvH) filling as a measure for the emergence of vHs physics in the honeycomb model (Figure 2(a)). The decreasing DoS at lvH filling, as a function of t_2 (cf. Figure 1(d)), directly translates to the fluctuation strength. However, the fluctuation spectrum appears to be much more susceptible to a violation of the perfect nesting condition: a slight detuning from perfect vHs filling leads to a substantial decrease in the fluctuation strength, as exemplified for two fixed values of t_2 in Figure 2(a). Accordingly perfect nesting plays the primary role in the emergence of electronic order rather than the decay of DoS associated with increasing t_2 .

Many-body analysis at the compensated metal crossover. We demonstrate compensated metal ordering tendencies when the single particle states in Eq. 1 are subjected to Hubbard interactions. We model many-body effects within the *random phase approximation* (RPA) [27–31], which focuses on collective particle-hole (ph) excitations as a driver of symmetry breaking transitions. Under this assumption, the full hierarchy of electronic screening processes can be cast into a geometric series that is evaluated analytically. This dresses the ph susceptibility in Eq. 2 to yield the RPA response functions

$$\chi_{c/s}^{\text{RPA}}(\mathbf{q}) = [1 \pm \chi^0(\mathbf{q}) U]^{-1} \chi^0(\mathbf{q}) \quad (3)$$

for charge and spin excitations, respectively. These quantities allow us to probe ph instabilities indicated by a divergent susceptibility channel. At lower scales, however, the RPA provides ph screening for the effective Cooper pair interaction

$$\Gamma(\mathbf{k}, \mathbf{k}') = U + U \chi^{\text{RPA}}(\mathbf{k} - \mathbf{k}') U - U \chi^{\text{RPA}}(\mathbf{k} + \mathbf{k}') U, \quad (4)$$

which can be evaluated within mean field theory at the Fermi level to reveal the resulting superconducting fluctuations [27]. The presented results are also found to be in

accordance with *functional renormalization group* (FRG) calculations [32–34]. As a direct consequence of Eq. 3 and the absence of sublattice interference on the honeycomb lattice, the charge response is suppressed by a repulsive interaction $U > 0$, and magnetic fluctuations dominate the low energy physics [11]. For χ_s^{RPA} , the higher order screening processes generally increase the imbalance between different momentum channels in the susceptibility. For sufficient interaction scales, χ_s^{RPA} diverges in correspondence to a generalized Stoner criterion, resulting in a spin density wave (SDW) transition.

We presume a generic instability analysis in a small energy window ΔE around the lower vHs in the presence of chiral symmetry breaking and charge compensation. Considering previous studies of the honeycomb Hubbard model [10, 11, 13, 35], that consistently find a SDW directly at vH filling, as well as the parameter range suitable for RPA studies, we fix the interaction scale to an intermediate value of $U = 1.5t_1$ to study the effect of electronic correlations around the Lifshitz transition to compensated metallicity. The landscape of symmetry broken phases around lower vH in Figure 2(b) is dominated by a superconducting phase which transforms according to the E_2 irreducible representation (irrep), displayed in Figure 2(c). The energetically favorable chiral superposition of its two dimensional order parameter gaps out regions of high DoS, *i.e.* areas in the vicinity of the M points [35]. Our findings agree with previous numerical studies of the $t_2 = 0$ honeycomb lattice near vH filling and indicate a chiral d -wave SC [10–12], which remains unaltered in the compensated metal regime. Indicated by its small amplitude the ep barely participates in the pairing process.

While the electronic fluctuation spectrum continues to be dominated by the nesting of the hp, the small Fermi velocity of the ep right above the pocket opening leads to a large DoS at the Fermi level centered around Γ . In this region, the available condensation energy for gapping out the central pocket competes with the electronic fluctuation scales of the hp. A competing s_{\pm} SC state (cf. Figure 2(c)) arises close to the pocket opening and is eventually superseded by the E_2 state at sufficient depth of quadratic band dispersion at Γ . Since we are interested in the scenario close to pristine filling around $t_2 \sim 0.85t_1$ this competitive regime can be safely neglected, and vH-type DoS is identified as the main driver for symmetry breaking in the investigated region of parameter space.

Conclusion and outlook For electronic honeycomb lattice models we find strong chiral symmetry breaking due to next-nearest neighbor hopping t_2 as a decisive parameter to tune the filling of the hole-like van-Hove level. The compensating electron-like circular FS pocket in the BZ center due to the Lifshitz transition implied by t_2 does not significantly participate in the symmetry breaking mechanism via many-body effects. Investigating the ordering tendencies of our honeycomb model around half filling with a hole pocket at van-Hove level, we obtain the sought

after chiral topological superconducting $d + id$ instability at pristine filling or for moderate doping achievable through methods such as electrolytic gating.

Facing graphene with $t_2/t_1 \sim 0.15$ [8] as the most tangible electronic honeycomb layer material, this raises the question of how to increase this ratio to the proposed high values $\gtrsim 0.8$ required to obtain vH physics at pristine filling. Buckling due to lattice mismatch in the growing process or z -elongated orbital contributions to the low energy theory can lead to a sufficient increase of long range hybridization, *e.g.* as reported for germanene [36, 37], while orbital-selective inter-layer hybridization with a substrate or other van-der-Waals (vdW) materials can also promote indirect long range tunneling via external electronic states [38–40]. Another avenue towards strong intra-sublattice hopping on the Honeycomb lattice is the realization of large Wannier orbitals like the Fidget spinner states originating from a topological obstruction, that omit the exponential localization of Wannier states at a single lattice site [41].

In this work we discuss chiral symmetry breaking via long ranged hybridisation as one mediator inducing compensated metallicity on the honeycomb lattice. However, the presented results rely on the systems fermiology rather than the detailed mechanism of charge compensation. Phenomenologically, this puts compensated metal tuning on the map of correlated quantum material design, which might render itself relevant for future endeavors in stacked multi-layer vdW materials [42, 43].

Acknowledgement. We thank J. Heßdörfer, and F. Reinert for discussions. The work is funded by the Deutsche Forschungsgemeinschaft (DFG, German Research Foundation) through Project-ID 258499086 - SFB 1170, and through the research unit QUAST, FOR 5249, project ID 449872909, and through the Würzburg-Dresden Cluster of Excellence on Complexity and Topology in Quantum Matter – *ct.qmat* Project-ID 390858490 - EXC 2147. We acknowledge HPC resources provided by the Erlangen National High Performance Computing Center (NHR@FAU) of the Friedrich-Alexander-Universität Erlangen-Nürnberg (FAU). NHR funding is provided by federal and Bavarian state authorities. NHR@FAU hardware is partially funded by the DFG – 440719683. M.D. received funding from the European Research Council under Grant No. 771503 (TopMech-Mat).

* Corresponding author: rthomale@physik.uni-wuerzburg.de

- [1] E. C. Stoner, Collective electron ferromagnetism, *Proceedings of The Royal Society A: Mathematical, Physical and Engineering Sciences* **165**, 372 (1938).
- [2] J. Bardeen, L. N. Cooper, and J. R. Schrieffer, Theory of superconductivity, *Phys. Rev.* **108**, 1175 (1957).

- [3] A. Consiglio, T. Schwemmer, X. Wu, W. Hanke, T. Neupert, R. Thomale, G. Sangiovanni, and D. Di Sante, Van hove tuning of av_3sb_5 kagome metals under pressure and strain, *Phys. Rev. B* **105**, 165146 (2022).
- [4] J. L. McChesney, A. Bostwick, T. Ohta, T. Seyller, K. Horn, J. González, and E. Rotenberg, Extended van hove singularity and superconducting instability in doped graphene, *Phys. Rev. Lett.* **104**, 136803 (2010).
- [5] P. Rosenzweig, H. Karakachian, D. Marchenko, K. Küster, and U. Starke, Overdoping graphene beyond the van hove singularity, *Phys. Rev. Lett.* **125**, 176403 (2020).
- [6] D. Haberer, L. Petaccia, A. V. Fedorov, C. S. Praveen, S. Fabris, S. Piccinin, O. Vilkov, D. V. Vyalikh, A. Preobrajenski, N. I. Verbitskiy, H. Shiozawa, J. Fink, M. Knupfer, B. Büchner, and A. Grüneis, Anisotropic eliashberg function and electron-phonon coupling in doped graphene, *Phys. Rev. B* **88**, 081401 (2013).
- [7] A. H. Castro Neto, F. Guinea, N. M. R. Peres, K. S. Novoselov, and A. K. Geim, The electronic properties of graphene, *Rev. Mod. Phys.* **81**, 109 (2009).
- [8] J. Jung and A. H. MacDonald, Tight-binding model for graphene π -bands from maximally localized wannier functions, *Phys. Rev. B* **87**, 195450 (2013).
- [9] Y. Hatsugai, T. Morimoto, T. Kawarabayashi, Y. Hamamoto, and H. Aoki, Chiral symmetry and its manifestation in optical responses in graphene: interaction and multilayers, *New Journal of Physics* **15**, 035023 (2013).
- [10] R. Nandkishore, L. S. Levitov, and A. V. Chubukov, Chiral superconductivity from repulsive interactions in doped graphene, *Nature Physics* **8**, 158 (2012).
- [11] M. L. Kiesel, C. Platt, W. Hanke, D. A. Abanin, and R. Thomale, Competing many-body instabilities and unconventional superconductivity in graphene, *Phys. Rev. B* **86**, 020507 (2012).
- [12] W. Wu, M. M. Scherer, C. Honerkamp, and K. Le Hur, Correlated Dirac particles and superconductivity on the honeycomb lattice, *Phys. Rev. B* **87**, 094521 (2013).
- [13] W.-S. Wang, Y.-Y. Xiang, Q.-H. Wang, F. Wang, F. Yang, and D.-H. Lee, Functional renormalization group and variational monte carlo studies of the electronic instabilities in graphene near $\frac{1}{4}$ doping, *Phys. Rev. B* **85**, 035414 (2012).
- [14] A. M. Alsharari and S. E. Ulloa, Inducing chiral superconductivity on honeycomb lattice systems, *Journal of Physics: Condensed Matter* **34**, 205403 (2022).
- [15] F. G. Ribeiro, E. P. Raposo, and M. D. Coutinho-Filho, Competing chiral d -wave superconductivity and magnetic phases in the strong-coupling hubbard model on the honeycomb lattice, *Phys. Rev. B* **107**, 064510 (2023).
- [16] O. Can, T. Tummuru, R. P. Day, I. Elfimov, A. Damascelli, and M. Franz, High-temperature topological superconductivity in twisted double-layer copper oxides, *Nature Physics* **17**, 519 (2021).
- [17] S. Wolf, T. Gardener, K. L. Hur, and S. Rachel, Topological superconductivity on the honeycomb lattice: Effect of normal state topology, *Phys. Rev. B* **105**, L100505 (2022).
- [18] A. Crépieux, E. Pangburn, L. Haurie, O. A. Awoga, A. M. Black-Schaffer, N. Sedlmayr, C. Pépin, and C. Bena, Superconductivity in monolayer and few-layer graphene. ii. topological edge states and chern numbers, *Phys. Rev. B* **108**, 134515 (2023).
- [19] J. M. Luttinger and J. C. Ward, Ground-state energy of a many-fermion system. ii, *Phys. Rev.* **118**, 1417 (1960).
- [20] J. M. Luttinger, Fermi surface and some simple equilibrium properties of a system of interacting fermions, *Phys. Rev.* **119**, 1153 (1960).
- [21] G. F. Chen, Z. Li, D. Wu, G. Li, W. Z. Hu, J. Dong, P. Zheng, J. L. Luo, and N. L. Wang, Superconductivity at 41 k and its competition with spin-density-wave instability in layered $\text{ceo}_{1-x}\text{fxFeAs}$, *Phys. Rev. Lett.* **100**, 247002 (2008).
- [22] X. H. Chen, T. Wu, G. Wu, R. H. Liu, H. Chen, and D. F. Fang, Superconductivity at 43 k in $\text{smfeso}_{1-x}\text{fx}$, *Nature* **453**, 761 (2008).
- [23] M. Rotter, M. Tegel, and D. Johrendt, Superconductivity at 38 k in the iron arsenide $(\text{ba}_{1-x}\text{kx})\text{fe}_2\text{as}_2$, *Phys. Rev. Lett.* **101**, 107006 (2008).
- [24] A. V. Chubukov, D. V. Efremov, and I. Eremin, Magnetism, superconductivity, and pairing symmetry in iron-based superconductors, *Phys. Rev. B* **78**, 134512 (2008).
- [25] S. Maiti and A. V. Chubukov, Renormalization group flow, competing phases, and the structure of superconducting gap in multiband models of iron-based superconductors, *Phys. Rev. B* **82**, 214515 (2010).
- [26] A. Chubukov, Pairing mechanism in fe-based superconductors, *Annual Review of Condensed Matter Physics* **3**, 57 (2012).
- [27] M. Dürrnagel, J. Beyer, R. Thomale, and T. Schwemmer, Unconventional superconductivity from weak coupling - a unified perspective on formalism and numerical implementation, *The European Physical Journal B* **95**, 112 (2022).
- [28] T. Takimoto, T. Hotta, and K. Ueda, Strong-coupling theory of superconductivity in a degenerate hubbard model, *Phys. Rev. B* **69**, 104504 (2004).
- [29] K. Kubo, Pairing symmetry in a two-orbital hubbard model on a square lattice, *Phys. Rev. B* **75**, 224509 (2007).
- [30] S. Graser, T. A. Maier, P. J. Hirschfeld, and D. J. Scalapino, Near-degeneracy of several pairing channels in multiorbital models for the fe pnictides, *New Journal of Physics* **11**, 025016 (2009).
- [31] M. Altmeyer, D. Guterding, P. Hirschfeld, T. A. Maier, R. Valentí, and D. J. Scalapino, Role of vertex corrections in the matrix formulation of the random phase approximation for the multiorbital hubbard model, *Physical Review B* **94**, 214515 (2016).
- [32] M. Bunney *et al.*, In preparation (2024).
- [33] W. H. C. Platt and R. Thomale, Functional renormalization group for multi-orbital fermi surface instabilities, *Advances in Physics* **62**, 453 (2013).
- [34] J. Beyer, J. B. Hauck, and L. Klebl, Reference results for the momentum space functional renormalization group, *The European Physical Journal B* **95**, 65 (2022).
- [35] A. M. Black-Schaffer and C. Honerkamp, Chiral d -wave superconductivity in doped graphene, *Journal of Physics: Condensed Matter* **26**, 423201 (2014).
- [36] A. Acun, L. Zhang, P. Bampoulis, M. Farmanbar, A. Houselt, A. Rudenko, M. Lingenfelder, G. Brocks, B. Poelsema, M. Katsnelson, and H. Zandvliet, Germanene: The germanium analogue of graphene, *Journal of physics. Condensed matter : an Institute of Physics journal* **27**, 443002 (2015).
- [37] D. Di Sante, X. Wu, M. Fink, W. Hanke, and R. Thomale, Triplet superconductivity in the dirac semimetal germanene on a substrate, *Phys. Rev. B* **99**, 201106 (2019).
- [38] H. Coy Diaz, J. Avila, C. Chen, R. Addou, M. Asensio, and M. Batzill, Direct observation of interlayer hybridiza-

- tion and dirac relativistic carriers in graphene/mos 2 van der waals heterostructures, [Nano letters](#) **15** (2015).
- [39] H. C. Diaz, Y. Ma, S. Kolekar, J. Avila, C. Chen, M. C. Asensio, and M. Batzill, Substrate dependent electronic structure variations of van der waals heterostructures of mose2 or mose2(1x)te2x grown by van der waals epitaxy, [2D Materials](#) **4**, 025094 (2017).
- [40] Y. Qu, Y. Xu, B. Cao, Y. Wang, J. Wang, L. Shi, and K. Xu, Long-range orbital hybridization in remote epitaxy: The nucleation mechanism of gan on different substrates via single-layer graphene, [ACS Applied Materials & Interfaces](#) **14** (2022).
- [41] H. C. Po, L. Zou, A. Vishwanath, and T. Senthil, Origin of mott insulating behavior and superconductivity in twisted bilayer graphene, [Phys. Rev. X](#) **8**, 031089 (2018).
- [42] E. Y. Andrei and A. H. MacDonald, Graphene bilayers with a twist, [Nature Materials](#) **19**, 1265 (2020).
- [43] T. Devakul, V. Crépel, Y. Zhang, and L. Fu, Magic in twisted transition metal dichalcogenide bilayers, [Nature Communications](#) **12**, 6730 (2021).